Magnetic resonance imaging: A potential tool in assessing the addition of hyperthermia to neoadjuvant therapy in patients with locally advanced breast cancer

OANA I. CRACIUNESCU[1], **DONALD E. THRALL**[2], **ZELJKO VUJASKOVIC**[1], and **MARK W. DEWHIRST**[1]

[1] Department of Radiation Oncology, Duke University Medical Center, Durham, North Carolina

[2] Department of Molecular Biomedical Sciences, College of Veterinary Medicine, North Carolina State University, Raleigh, North Carolina

Abstract

The poor overall survival for patients with locally advanced breast cancers has led over the past decade to the introduction of numerous neoadjuvant combined therapy regimens to down-stage the disease before surgery. At the same time, more evidence suggests the need for treatment individualisation with a wide variety of new targets for cancer therapeutics and also multi modality therapies. In this context, early determination of whether the patient will fail to respond can enable the use of alternative therapies that can be more beneficial. The purpose of this review is to examine the potential role of magnetic resonance imaging (MRI) in early prediction of treatment response and prognosis of overall survival in locally advanced breast cancer patients enrolled on multi modality therapy trials that include hyperthermia. The material is organised with a review of dynamic contrast (DCE)-MRI and diffusion weighted (DW)-MRI for characterisation of phenomenological parameters of tumour physiology and their potential role in estimating therapy response. Most of the work published in this field has focused on responses to neoadjuvant chemotherapy regimens alone, so the emphasis will be there, however the available data that involves the addition of hyperthermia to the regimen will be discussed The review will also include future directions that include the potential use of MRI imaging techniques in establishing the role of hyperthermia alone in modifying breast tumour microenvironment, together with specific challenges related to performing such studies.

Keywords

imaging (DCE-MRI-DW-MRI); locally advanced breast cancer; physiological effects of hyperthermia; prediction and monitoring of tumour response

Introduction

Before the neoadjuvant therapy era, the prognosis for patients with locally advanced breast cancer (LABC) was poor, with a five-year overall survival of 55% [1–3]. The five-year survival of patients with inflammatory disease was even lower, at 15% [4]. To improve

Correspondence: Oana I. Craciunescu, PhD, DABR, Box 3295, Duke University Medical Center, Durham, NC, 27710, USA. Tel: (919) 660-2192. Fax: (919) 681-6183. oana.craciunescu@duke.edu.

outcome, a multidisciplinary, neoadjuvant approach has been employed. Despite relatively high clinical response rates (70–98%), and pathological complete response in a subgroup of patients (3–34%) [5–8], this approach did not lead to improved overall or disease-free survival. Patients receiving neoadjuvant chemotherapy had better local control and a higher breast conservation rate [9,10]. Importantly, patients with a pathological complete response (pCR) appeared to have improved overall survival. The rate of pCR in patients with T1–3 breast cancer receiving anthracycline-based chemotherapy is about 13% [10]. In more advanced breast cancers (i.e. T4), the response rates are likely to be even lower Although the addition of taxanes increased the pCR to about 26% in patients with T1–3 breast cancer, there is obviously considerable room for improvement [11].

Hyperthermia has a number of potentially beneficial antitumour effects when combined with chemotherapy that can result in improved response. At temperatures >41°C, there is increased tumour blood flow [12,13], which can result in increased drug delivery [14]. To further enhance drug activity at elevated temperature, the combination of HT and liposome encapsulated drugs has been investigated extensively [15]. HT increases liposome extravasation into tumours, leading to increased intratumoural drug concentration [15,16].

An additional advantage of combining HT with chemotherapeutic agents (including doxorubicin) is that they exhibit enhanced cell killing at elevated temperature [17,18]. The therapeutic benefits from liposomes and hyperthermia individually, coupled with the potential advantages seen by their combination, make the use of the two modalities together an attractive method for drug delivery to tumours. Thus, a phase I/II study to describe safety/ tolerability and determine the response of a novel combination treatment of paclitaxel, liposomal doxorubicin (Evacet™) and local hyperthermia in patients with locally advanced breast cancer in the preoperative setting was proposed and completed [11]. A total of 47 patients were enrolled onto this study (21 and 26 patients in phase 1 and 2, respectively), with 43 evaluable patients. Four patients, 9%, 95% confidence interval (CI), 0.6% to 18%, achieved a pathologic complete response following neoadjuvant treatment. Combined (partial + complete) clinical response rate was 72% (95% CI, 58.6% to 85.4%), and combined pathologic response rate was 60% (95% CI, 45.4% to 74.6%). Eight patients elected to have breast-conserving surgery out of 16 patients that were eligible for this more conservative option following neoadjuvant treatment. These results are encouraging, particularly given that the patient population had mostly T3 or T4 tumours, with 32% of the enrolled patients having inflammatory cancer (T4d) [11]. The reported 26% pCR rates with taxane-based chemotherapy in past studies were in more favourable patients with T1-3 tumours. Furthermore, despite the more advanced disease in these patients, the five-year disease-free survival rates were similar to the 89% reported for stage II breast cancer [19].

Even more dramatic results are expected as a low temperature sensitive liposome (LTSL) has been developed, which releases its content in a matter of seconds in the vasculature of the heated volume, at clinically achievable temperatures [20,21]. The intratumoural doxorubicin (DOX) concentration resulting from a LTSL + HT is 20–30 times higher than with systemic administration of free doxorubicin [22]. This opened up an entirely new field where HT could be used to target the release of drug into the tumour vasculature, and simultaneously enhance its effect [23].

With any technically complex cancer treatment modality, identification of patients likely to respond is important. Refractory patients should not be treated. Currently, it is impossible to distinguish between HT-refractory versus HT-responsive tumours, either in chemotherapy or radiation therapy settings. Individualisation of patient therapy could be based on genomic properties [24], but tumour physiological parameters and tumour imaging can also be used as predictors, and such parameters may provide information distinct from the genomic

phenotype [25,26]. Functional imaging techniques that have shown potential in early assessment to respond to neoadjuvant therapies, in breast and other cancers, include magnetic resonance-based imaging techniques such as dynamic contrast enhanced (DCE)-MRI, diffusion weighted (DW)-MRI and magnetic resonance spectroscopy (MRS), nuclear medicine sestamibi imaging using 99m Tc, and positron emission tomography (PET) techniques [27].

The purpose of this review is to examine the potential role of magnetic resonance imaging (MRI) in early prediction of treatment response and prognosis of overall survival in locally advanced breast cancer patients enrolled on multi modality therapy trials that include hyperthermia. The material is organised with a review of dynamic contrast (DCE)-MRI and diffusion weighted (DW)-MRI for tumour physiology characterisation and therapy response purposes. The review will also include future directions that include the potential use of MRI imaging techniques in establishing the role of hyperthermia alone in modifying breast tumour microenvironment, together with specific challenges related to performing such studies.

DCE-MRI

Dynamic contrast-enhanced (DCE)-MRI is a non-invasive technique to study tumour vascularity and allows quantification of the model parameters. It is a useful technique for a wide range of clinical applications such as screening for malignant disease, tumour staging and has also the ability to measure treatment induced changes in tumour physiology which occur early in the course of treatment, prior to any observable anatomical changes [28,29]. It therefore has the potential to detect response and/or non-response to therapy which could permit the treatment to be adapted.

DCE-MRI, used commonly to quantify tumour perfusion/permeability related parameters, involves intravenous bolus injection of a low-molecular weight contrast agent followed by rapid image acquisition to measure signal enhancement over time as the contrast agent travels into and through the tumour vasculature. The only class of approved paramagnetic contrast agents in clinical use are low-molecular-mass Gd-based agents such as Gadopentate dimeglumine, Gd-DTPA (Magnevist®), Gadodiamide (Omniscan®), Gadobenic acid (Multihance®), Gadoteridol Gd-HP-DO3A (Prohance®), Gadofosveset (Ablavar®), Gadoversetamide (OptiMARK®), Gadoxetic acid (Eovist®, Primovist®) [30]. The contrast agent preferentially accumulates in tumour due to increased perfusion and increased vessel permeability. Early accumulation of contrast agent likely reflects increased or altered vascularity [31]. Based on human trials, the increase in signal after contrast agent arrival relates to vascular density and the rate of enhancement characterises vascular fenestration and functional permeability [32]. The interstitial environment influences the diffusivity and temporary retention (wash-out) of the contrast agent, i.e. tumours with high cellularity/ packing don't have a large extracellular space for the contrast agent to distribute, hence it returns rapidly to the blood stream [33–35].

There exists an inherent trade off in dynamic sequences between spatial resolution, temporal resolution and anatomical coverage. In DCE-MRI high spatial resolution images which cover the whole tumour extent are needed for detailed analysis of the lesion structure. At the same time, high temporal resolution is required to allow accurate assessment of kinetic features. A second reason for the high temporal resolution requirement is that analysis of subtle morphological features is only feasible following soon after contrast injection as this is when the lesion-to-parenchyma contrast is optimal [36]. However, improved spatial resolution is achieved at the cost of poorer temporal resolution. Because of this trade off, fast T_1-weighted spoiled gradient echo sequences are often the preferred method because

they allow good contrast medium sensitivity, high signal-to-noise ratio, adequate anatomical coverage and rapid data acquisition and are also easy to evaluate as compared to saturation or inversion prepared gradient echo sequences [37]. In terms of new acquisition methods there has been considerable effort in introducing more effective fat suppression for dynamic MRI and faster acquisition sequences that balance the need for both high spatial and temporal resolution. The interested reader is referred to a recent review by Sinha and Sinhaon advances in breast MRI and MRS [28].

Signal enhancement in DCE-MRI

After the contrast agent is administered, it quickly diffuses into and out of the interstitial space. The signal enhancement reflects flow and volume of blood and typically occurs in three stages in all tissues. There is an initial increase in enhancement due to contrast leakage from the blood vessels to interstitial space (wash-in). This is followed by an equilibrium state where net passage of contrast between the two compartments is stable (plateau). Finally, there is a net increase in the reverse flow of contrast into the blood vessels from the interstitial space (wash-out). As mentioned, greater signal enhancement is observed in the tumour as compared with normal tissue because of the high perfusion and increased vessel density and also due to the highly permeable, leaky nature of the tumour microvasculature. However, DCE-MRI reveals functional diversity of the vasculature in both malignant and benign lesions, making it ideal for screening for malignant disease. Care has to be taken as benign lesions can display higher (breast fibroadenomas [38]) or similar (benign prostatic hyperplasia [39]) enhancement rates than malignant lesions.

The extent of signal enhancement depends on tissue perfusion, arterial input function (AIF – the concentration-time course of contrast agent in the artery that supplies the vascular bed), capillary surface area, capillary permeability and the volume of the extracellular extravascular interstitial space (EES) [40–45]. T_1-weighted DCE-MRI analysis is able to generate parameters that represent one of, or combinations of these processes, and can be used to measure abnormalities in tumour vessel flow, blood volume and permeability [40].

MRI-extracted physiological parameters

Signal enhancement assessment methods are either semi-quantitative (or model-free quantifications) which analyse signal intensity changes, or quantitative (or model-based). Three major quantitative models have been reported by Larson et al. [46], Brix et al. [47] that models signal intensity with the assumption that signal intensity changes are proportional to contrast agent concentration changes, and by Tofts et al. [48] that models directly the change in concentration of the contrast agent. These methods have been reconciled by Tofts in 1997 [49] and standardised terminology and guidelines were set by Tofts et al. in 1999 [50]. These pharmacokinetic models are based on the concept of tissue compartmentalisation. Tissue can be described as comprising of three compartments: vascular plasma space, extracellular extravascular space (EES), and intra-cellular space [48].

The most popular PK model is the Tofts model which uses just such a compartment model to determine the change in tissue concentration of the contrast agent with time, and relates it to the signal enhancement seen in the MR images [48,51]. It was initially developed to measure blood–brain barrier permeability and leakage space, and later was modified for analysis of breast lesions [48] and other tissues [52–54], and is one of the current standards for DCE-MRI analysis [50]. This model describes the contrast agent exchange between the main blood compartment, whole body extracellular space, lesion leakage space and the contrast agent leakage through kidneys. Three contrast agent kinetic parameters, the vascular transfer function (K^{trans}), extracellular extravascular volume fraction (v_e), and the rate constant (k_{ep}) have potential to quantify treatment induced changes. The parameter of

greatest interest is K^{trans}, since it is the parameter associated with microvascular physiology [55], perfusion as reflects contrast delivery and permeability as reflects transport across the vascular endothelium [29].

The longitudinal relaxation time before contrast administration, T_{10}, is a very important parameter in the Tofts-based pharmacokinetic analysis. The accuracy with which parameters such as K^{trans} and v_e follow vascular properties is dependent on the use of imaging methods that allow T_{10} calculation, and when such techniques are used, the parameters closely relate to tissue properties [56]. Consensus recommendations for DCE-MRI [57]underlined the necessity of acquisition of raw data for the purpose of calculating special maps of precontrast longitudinal relaxation times. Dale et al. [55] summarise the two most commonly used methods for measuring longitudinal relaxation: a dual spin echo technique with variable T_R, and the variable flip angle technique.

Due to the assumptions made [49], any of the compartmental models provide only a phenomenological description of the contrast media transport and volume fractions. The true values might substantially differ from the value determined by using DCE-MRI.

In order to avoid some challenges related with PK modeling including computational time, post-processing inaccuracies, and fit failures, non-model-based parameters are often used in addition to or in place of model-based methods. One of the simplest model-free quantification models is an integration of the concentration of the contrast agent observed over time, the initial area under the concentration-time curve iAUC [mmol] [58]. The value of iAUC is dependent on the period over which integration is performed, typically between the contrast agent administration and a time t after the start time. As summarised by Walker-Samuel et al. [59], changes in iAUC and other non-model-based parameters (peak enhancement, wash-in/wash-out gradients) have been shown to correlate with tumour regression rates. Semi-quantitative methods are easier to calculate, but they suffer numerous limitations including the fact that they do not accurately reflect the vascular endpoints of interest namely tissue perfusion, blood volume and vascular permeability [60]. Other important limitation of semi-quantitative (or model-free quantification) models is their dependence on parameters such as the rate of injection, field strength, pulse sequence, gain and scaling factors that usually vary from scanner to scanner, making it hard to compare between studies [29].

The review by Parker and Buckley [37] describes in detail, from basics to more challenging modeling the approaches used in tracer kinetic modeling for T_1-weighted DCE-MRI. Another important resource for use of DCE-MRI extracted parameters to assess changes in tumour physiology and assessment of response is the workshop review by Leach et al. [29], and for readers of this journal the review by Ludemann, Wust and Gellerman [61].

Clinical applications: Breast imaging

Potential clinical applications of DCE-MRI include screening for malignant disease, lesion characterisation, determining tumour physiology (tumour perfusion, microvascular vessel wall permeability and extracellular volume fraction), monitoring treatment response, and assessing for residual disease [28,56].

Newer applications include disease prognosis, assessing efficacy of antivascular anticancer drugs, and predicting treatment response [28]. For example, owing to the role of angiogenesis in tumour growth, anti-angiogenic and vascular disrupting drugs have been developed over the last 10–15 years to target the cluster of tiny new blood vessels created during angiogenesis [62]. Specifically, many anti-angiogenic drugs target the angiogenic cytokine VEGF, a principal mediator of vascular permeability, which can be measured by

DCE-MRI [63]. With the development of anti-angiogenic agents, many of which are now undergoing clinical trials, there is an increased need to monitor tumour microvasculature, and by so doing, evaluate the effectiveness of these therapies [29]. Unlike chemotherapy and radiotherapy, where the goal is to destroy cancer cells, anti-angiogenic agents prevent the formation of new vessels and disrupt any networks of abnormal capillaries that feed the tumour [64]. By limiting tumour blood supply in this way, these agents shrink tumours and prevent their growth.

The potential of DCE-MRI to evaluate response of LABC patients to neoadjuvant chemotherapy has been examined [65–70]. Results indicate that changes in contrast agent kinetics can be used to evaluate chemotherapy regimens and predict final clinicopathologic response. For example, in invasive breast cancer the presence of a rim enhancement pattern, early maximal enhancement and washout phenomena were independently associated with the poor prognostic indicators of higher histological grade, more rapid cellular proliferation measured using Ki-67 (an immunohistochemically detected biomarker of proliferation), and negative estrogen receptor status [71]. In another study, the internal composition of responding tumours changed from heterogeneous to homogeneous and there was a decrease in peak enhancement [72]. Also, in inflammatory breast cancer treated with bevacizumab, contrast medium inflow transfer rate constant and extracellular volume fraction decreased after bevacizumab alone [35]. Similarly, as reported by Baar et al. [73], the anti-vascular endothelial growth factor (VEGF) antibody, bevacizumab, has resulted in a greater reduction in tumour perfusion when added to docetaxel, then docetaxel alone. Semi-quantitative parameters like the relative signal intensity and initial area under the curve were used to predict survival and early clinical response to primary chemotherapy in patients with LABC [74]. They concluded that DCE-MRI in LABC has the potential to predict 5-year survival and also assess changes in tumour vascularisation after just one cycle.

Applications to hyperthermia

Several studies have looked at the potential use of DCE-MRI to estimate the success of high-intensity focused ultrasound (HIFU) ablation of breast tumours. Knowing the increased sensitivity of DCE-MRI to detect residual disease, the studies investigated several imaging features like signal intensity change and enhancement pattern in breast cancer patients undergoing HIFU [75–77]. Hence, these studies used the diagnostic capabilities and advantages of DCE-MRI to establish the efficacy of a novel treatment.

The only study to date that demonstrated the potential role for DCE-MRI extracted parameters to estimate response to neoadjuvant therapies in LABC patients that included hyperthermia was that of Craciunescu et al. [78]. The authors combined pre treatment MR derived parameters into a Morpho-Physiological Tumour Score (MPTS) that allowed prediction of outcome in LABC patients treated with neoadjuvant chemotherapy and HT. Combining information about the tumour enhancement pattern (morphology information) with information extracted from a semi-quantitative analysis of time/intensity curves of the contrast agent, wash-in and wash-out parameters related to physiological information, the MPTS predicted response with a sensitivity of 91%, and a specificity of 78%. This system of tumour characterisation can also be expanded for treatment outcome scoring. The assumption is that with responders, the enhancement velocity gets smaller, i.e., the wash-in parameter gets smaller. The concept was tested for correlation with treatment response on two case studies [79]. Figure 1 shows two examples of this approach. The first is in stage IV disease, which responded completely. First row in Figure 1a) shows raw DCE-MR images taken pre-cycle I, pre-cycle II and pre-surgery, and the second row shows generated wash-in maps. The MPTS score pre-cycle I was a maximum of 6. The MPTS score remained 6 throughout the treatment. The morphology score was not determined in the pre-surgery

images, as no residual tumour was found by imaging means. The second is in stage III disease with axillary involvement, which did not respond. First row in Figure 1b) shows raw DCE-MR images taken pre-cycle I, pre-cycle II and pre-surgery, and the second row shows generated wash-in maps. The MPTS score pre-cycle I was 1. The MPTS score remained at 1 for the pre-cycle II data, as the wash-in parameter increased only slightly, not changing the score. The association between MPTS score and outcome in this study, illustrated by Figure 1, paved the way for another LABC trial (see Future Directions).

Although not applied directly to breast imaging, an excellent review on DCE-MRI and its implications in hyperthermia by Ludeman, Wust and Gellerman was published in this journal [61]. The authors describe and recognised the main challenges in using DCE-MRI for tissue perfusion characterisation: 'To assess perfusion changes due to hyperthermia using DCE-MRI one has to take into account the systematic variation of the arterial input function required for perfusion quantification. Hyperthermia modifies the contrast agent bolus in that a shorter and more highly concentrated bolus appears earlier in the tissue.' Thus, for quantitative extraction of PK parameters and their use to estimate changes due to hyperthermia, it is mandatory 'to normalise perfusion estimation to an individual AIF' [61]

DW-MRI

Diffusion-weighted magnetic resonance imaging (DW-MRI) is a specialised technique that measures the degree of diffusion of water molecules within extracellular space and between intracellular and extracellular space [80]. In DW-MRI, the MR signal is attenuated due to the thermally driven motion of water molecules affording an insight into tissue microstructure [81]. The diffusion of water in tissue is strongly affected by fluid viscosity and membrane permeability between intracellular and extracellular components, active transport and flow, and directionality of structures that impede or enhance mobility [28].

Each diffusion-weighted series is comprised of at least two diffusion-weighted images that are differently sensitised to diffusion, say signal intensity S_o recorded for $b_0 = 0$ s/mm^2, and signal intensity S recorded at a high b. The b-value is determined solely by diffusion gradient strengths and timings [82]. The apparent diffusion coefficient (ADC) is calculated as:

$$ADC = \frac{1}{b - b_0} \log\left(\frac{S_{b0}}{S_b}\right)$$

(1)

ADC provides a quantifiable measure of the signal attenuation and, therefore, the molecular motion of water. The ADC is high in tissues with few obstacles to the motion of water, whereas ADC is low in tissues with many obstacles. Quantifying the apparent diffusion coefficient (ADC) of water is a rapid, routine imaging sequence making it clinically attractive. The low b-values typically used (<1000 s/mm^2) assess diffusions in the interstitial space. A decreased diffusion is typically found at infarcted areas at the brain where the cells are swollen and the interstitial space reduced. An increased diffusion is found in necrotic tumour areas with increased interstitial space due to cell degeneration. Therefore an increased interstitial volume can be assessed by using diffusion MRI showing increase diffusibility as well as by DCE-MRI showing an increase leakage space [83].

Under conditions of high b-values or short diffusion time it is possible to demonstrate marked deviations from the mono-exponential equation that allows for ADC calculation using Equation 1. A significant decrease in ADC was demonstrated for human brain tissue using diffusion times between 40 and 800 ms, and b-values up to about 2200 s/m [84].

Alternatively, the data can be fitted by a bi-exponential curve with an intracellular and an extracellular compartment model [85].

Diffusion MRI is sensitive to structure at cellular level, thus has the potential to detect and quantify cellular changes that occur in response to successful therapies [86]. Intracellular water is tightly bound and high density cellular packing in cancers has low diffusivity. During an effective treatment, cancerous cells are killed, increasing the ADC in those areas. ADC has been demonstrated to be inversely correlated to cellular density [86–89].

Originally implemented to characterise acute cerebral infarction, diffusion-weighted MRI has also found application to assess response and as a predictor of outcome following or during cancer therapy of brain tumours [81,90,91], rectal carcinomas [92–95] hepatic metastasis [96], and cervical cancer [97].

Increases in the ADC early in treatment have been associated with more favourable outcome, with increased ADC thought to signify greater cell killing leading to less restricted water diffusion [98,99]. Diffusion-weighted imaging in concert with standard spin-echo sequences can also be used to characterise the physical makeup of a tumour, such as tightly packed cellularity versus fibrous tissue, versus liquefactive necrosis [100].

In breast imaging, a comprehensive review of the use of DW-MRI for both screening and treatment monitoring was published by Sinha and Sinha [28]. Theilmann et al. [101] showed in a study involving thirteen subjects with metastatic breast cancer, that changes in ADC values can predict response to treatment as early as 4 to 11 days after the start of treatment. Pickles et al. [102] determined that DW-MRI may provide a suitable biomarker capable of providing an indication of response to treatment prior to tumour size measurements. The first integration of quantitative DCE-MRI and ADC mapping to monitor treatment response in LABC treated with neoadjuvant therapy was reported by Yankeelov et al. [102]. They showed that their analysis is sensitive to longitudinal changes in breast tumour status, with K^{trans} and ADC being the most sensitive to these changes. Although limited by several factors related to the imaging parameters and the small number of patients employed in their study, the relationships between parameters still provide information on water distribution and geometry in the tumour environment. Figure 2 shows pre-treatment and post-treatment parametric maps of T_1, K^{trans}, v_e, τ_i and ADC of the central slice of the tumour from a representative patient, with τ_i representing the average intracellular water lifetime of a water molecule.

More recently, a voxel-by-voxel functional diffusion mapping for early evaluation of breast cancer treatments was reported by [103]. The DWI scans were acquired at three different time points: pre-, early post- and late post- treatment. Even with limited data sets they observed, after non-rigid registration of the three sets, that a correlation between changes of ADC values and treatment response exists.

Application to hyperthermia

The morphologic characterisation offered by ADC mapping could be valuable with reference to HT where the physical properties of the tissue may be altered directly by treatment. However, interpretation of ADC changes may not be as straightforward as in tumours treated with radiation or chemotherapy. Little is known about changes in the ADC following HT, other than in thermal ablation where the ADC decreased after treatment in prostate [104], but increased after treatment in transplanted carcinoma [105], and lung [98]. These data regarding the ADC and thermal ablation suggest that accepted paradigms of changes in ADC following therapy may depend on treatment modality and site. The absolute

temperature, which is relatively high in thermal ablation and in some regions of a tumour during non-ablative therapy, may also have an effect.

Image evaluation

Currently, the most frequently applied methods for DCE-MRI and ADC analysis include tracking changes during the course of treatment in the MR-extracted parameters obtained over a region or volume of interest (ROI/VOI), or by using histograms describing their distribution. Histogram-based methods are less user dependent, less arbitrary and provide a more reproducible tool for tumour assessment.

When averaging over ROI/VOI, their optimal depiction is not yet established and it is definitely site dependent, as some anatomical sites are more prone to motion than others. The diagnostic breast MR literature overwhelmingly reports the use of the most enhancing part of the ROI ('hot spot'), as it is thought that for diagnostic purposes the most aggressive component of the tumour, i.e. the highest enhancement, should be investigated [106–109]. For therapy response Hayes et al. [110] looked at differences in pharmacokinetic parameters in 15 LABC patients when the analysis was performed pixel-by-pixel, over the whole tumour and over a 'hot spot' showing that the whole ROI PK values are identical to the median values determined from histogram analysis of all pixels within the ROI. A greater range of changes was observed in the upper extremes of the histogram ('hot spots') compared to median values. More recently, Pickles et al. [65] have determined that analysis based on highly enhancing ROIs (so-called 'hot-spots') provided more statistically significant differences between responders and non-responders then the analysis based on ROI encompassing the whole tumour. For use of MR imaging for treatment response, the most comprehensive guidelines for ROI/VOI delineation come from the workshop review of Leach et al. [29] who give detailed recommendation.

However, both ROI/VOI analysis and histogram analysis are limited. ROI/VOI methods don't capture the tissue heterogeneity as observed in the MR-derived parameter values. Both methods discard information on spatial localisation. For this reason, voxel-to-voxel comparison methods are used that retain spatial information [111]. Such methods can provide unique insights into tumour structure, function and response [29] These methods require special software for results analysis and cannot be accurately used unless the images acquired at different stages throughout the treatment are correctly registered.

Image registration

Image registration is recommended [29] for any study that proposes to look at changes in imaging parameters with treatment response. Breast is a particularly challenging site from this point of view, as it consists of soft, deformable tissue that moves due to respiratory and cardiac cycles. First, registration is recommended to address any intrasessional movement caused by respiratory and cardiac motion and also any involuntary patient motion or muscle relaxation during the image acquisition, affecting any image analysis performed on such perturbed images. Automatic motion correction is an important pre-processing task for the analysis of MR images. Considerable research has been devoted to pre-processing image data to correct for misalignment due to motion artefacts. Reduction of such artefacts is thus fundamental for valid morphological or dynamic image analysis [28]. Motion correction is performed by the application of registration techniques to the dynamic image series. For breast DCE-MRI data, images are typically registered to the first post-contrast image, in order to avoid lesion degeneration. Tanner et al. [112] quantitatively evaluated several registration algorithms (rigid, affine, B-spline based non-rigid, single-resolution, multi-resolution, and volume-preserving) for the alignment of 3D DCE-MR images of the breast.

They evaluated that images were most accurately aligned with volume-preserving single-resolution non-rigid deformable registration using 40 or 20 mm control point spacing.

In addition, when images are acquired at different time points for evaluation of treatment response, there is large intersession motion due to patient repositioning and large deformations of the breast relative to previous imaging sessions. The latter are harder to deal with using rigid registration, and non-rigid (deformable) registration algorithms have been proposed. Li et al. [113] described a method where DCE-MRI data sets obtained in separate imaging sessions can be co-registered to a common image space, maintaining spatial information for voxel-by-voxel comparison. Non-rigid deformable registration using mutual information and warping was used for a voxel-by-voxel analysis of diffusion mapping for early evaluation of breast cancer treatment [103].

For hyperthermia applications, especially for studies that propose to look at the influences of heat treatments alone in the changes of tumour microenvironment, the need for registration is even more acute, as the pre- and post-HT treatment image sets have to be registered with the non-invasive MR temperature maps obtained during treatment. Similar patient positioning and immobilisation is crucial in attempting such a task.

Future directions

As described in the previous paragraphs, MRI-based parameters like k^{trans} and ADC have the potential to characterise the tumour microenvironment as surrogates for perfusion/permeability and cellularity. When these MR parameters are monitored before and after a hyperthermia treatment, without any other therapeutic intervention, i.e. chemotherapy or radiation, the effects of HT alone can be quantified and correlated with volumetric temperature distribution maps generated from non-invasive thermometry and consequently related to treatment outcome. This will allow, for the first time, a volumetric assessment of the effects of perfusion/permeability through K^{trans} changes and cell death through the apparent diffusion coefficient (ADC) on the resulting thermal distribution, and then a volumetric assessment of the effects of the temperature distribution on K^{trans} and ADC. Simple tracer kinetics models do not allow perfusion and permeability to be quantified separately. More advanced imaging and imaging analysis techniques have been proposed that can simultaneously quantify perfusion and permeability [114]. Also, novel imaging techniques have been proposed that simultaneously image tumour oxygenation and microvascular permeability [115]. Such technique has increased potential to select tumours that reflect treatment resistance. This new information will provide an opportunity to tailor the temperature distribution based on pretreatment physiological parameters, and to predict outcome based on changes in MR-extracted parameters following tumour heating. One important aspect that will have to be elucidated is the variability of the contrast longitudinal relaxation time (T_{10}) between the pre-HT DCE-MRI session, and the post-HT session and how these changes, if any, will affect the changes in the PK parameters.

These approaches are likely to lead to a new level of understanding of the effects of hyperthermia and a robust method for patient selection.

In breast therapy, such an analysis has several major challenges that relate to image acquisition and processing. For a more comprehensive voxel-to-voxel analysis, DCE/DW-MRI images will have to be registered between the time points (before and after HT) and with the MR temperature maps. The complexity of image registration for breast was described earlier. If an ROI technique is used, the choice of the ROI/VOI is also debated and several strategies in defining such regions for analysis might be necessary to establish the methodology that gives more statistically significant differences between responders and

non-responders, or separate the most the physiological parameters pre- versus post-HT treatment.

Conclusion

Breast imaging using MRI techniques is an area of wide interest and active research as treatment choices for breast cancer patients in general, and LABC patients in particular have become more and more individualised. It has been proven in the last decade that non-invasive MRI methods can have wide-ranging pre-clinical and clinical applications that are capable of providing spatial and temporal information about the tumour vasculature, metabolism and physiology. MR imaging has been proven to have great potential for lesion characterisation, from morphology with high dimensional structural imaging, perfusion/permeability with DCE-MRI, to cellularity with DWI, aiding in the development of novel targeted therapies, and also with great potential for early determination of response to treatment [28].

When hyperthermia is added to a neoadjuvant regimen, MR imaging offers the same potential in describing changes in the tumour microenvironment and in assessing early the response to treatment. It is likely that tumour physiological parameters such as tumour hypoxia, perfusion and cellularity, as assessed non-invasively using MRI and other imaging techniques, are related to the volumetric temperature distribution, as assessed with non-invasive MR temperatures, and are all linked to outcome. The ability to co-register these parameters volumetrically will offer a new paradigm for understanding the underlying mechanisms of hyperthermia. An exquisite model of the effects of temperature on the tumour, and the influence of pre-treatment and post-treatment variables on outcome, can be developed, with the net effect of optimising and maximising the use of hyperthermia in the fight against cancer.

References

1. Honkoop AH, van Diest PJ, de Jong JS, Linn SC, Giaccone G, Hoekman K, Wagstaff J, Pinedo HM. Prognostic role of clinical, pathological and biological characteristics in patients with locally advanced breast cancer. Br J Cancer 1998;77(4):621–626. [PubMed: 9484820]

2. Swain SM, Sorace RA, Bagley CS, Danforth DN Jr, Bader J, Wesley MN, Steinberg SM, Lippman ME. Neoadjuvant chemotherapy in the combined modality approach of locally advanced nonmetastatic breast cancer. Cancer Res 1987;47(14):3889–3894. [PubMed: 3036348]

3. Sataloff DM, Mason BA, Prestipino AJ, Seinige UL, Lieber CP, Baloch Z. Pathologic response to induction chemotherapy in locally advanced carcinoma of the breast: A determinant of outcome. J Am Coll Surg 1995;180(3):297–306. [PubMed: 7874340]

4. Lerebours F, Bieche I, Lidereau R. Update on inflammatory breast cancer. Breast Cancer Res 2005;7(2):52–58. [PubMed: 15743511]

5. Rastogi P, Anderson SJ, Bear HD, Geyer CE, Kahlenberg MS, Robidoux A, Margolese RG, Hoehn JL, Vogel VG, Dakhil SR, et al. Preoperative chemotherapy: Updates of National Surgical Adjuvant Breast and Bowel Project Protocols B-18 and B-27. J Clin Oncol 2008;26(5):778–785. [PubMed: 18258986]

6. Bonadonna G, Valagussa P, Brambilla C, Ferrari L, Moliterni A, Terenziani M, Zambetti M. Primary chemotherapy in operable breast cancer: Eight-year experience at the Milan Cancer Institute. J Clin Oncol 1998;16(1):93–100. [PubMed: 9440728]

7. Bear HD, Anderson S, Brown A, Smith R, Mamounas EP, Fisher B, Margolese R, Theoret H, Soran A, Wickerham DL, et al. The effect on tumor response of adding sequential preoperative docetaxel to preoperative doxorubicin and cyclophosphamide: Preliminary results from National Surgical Adjuvant Breast and Bowel Project Protocol B-27. J Clin Oncol 2003;21(22):4165–4174. [PubMed: 14559892]

8. Makris A, Powles TJ, Ashley SE, Chang J, Hickish T, Tidy VA, Nash AG, Ford HT. A reduction in the requirements for mastectomy in a randomized trial of neoadjuvant chemoendocrine therapy in primary breast cancer. Ann Oncol 1998;9(11):1179–1184. [PubMed: 9862047]

9. Mauri D, Pavlidis N, Ioannidis JP. Neoadjuvant versus adjuvant systemic treatment in breast cancer: A meta-analysis. J Natl Cancer Inst 2005;97(3):188–194. [PubMed: 15687361]

10. Mieog JS, van der Hage JA, van de Velde CJ. Neoadjuvant chemotherapy for operable breast cancer. Br J Surg 2007;94(10):1189–1200. [PubMed: 17701939]

11. Vujaskovic Z, Kim DW, Jones E, Lan L, McCall L, Dewhirst DW, Craciunescu O, Stauffer P, Liotcheva V, Betof A, Blackwell K. A Phase I/II Study of Neoadjuvant Liposomal Doxorubicin, Paclitaxel, and Hyperthermia in Locally Advanced Breast Cancer. International Journal of Hyperthermia 2010;26(5):514–521. [PubMed: 20377362]

12. Vujaskovic Z, Song CW. Physiological mechanisms underlying heat-induced radiosensitization. Int J Hyperthermia 2004;20(2):163–174. [PubMed: 15195511]

13. Dewhirst MW, Vujaskovic Z, Jones E, Thrall D. Re-setting the biologic rationale for thermal therapy. Int J Hyperthermia 2005;21(8):779–790. [PubMed: 16338861]

14. Hahn, G. Hyperthermia and Cancer. New York: Plenum Press; 1982.

15. Kong G, Dewhirst MW. Hyperthermia and liposomes. Int J Hyperthermia 1999;15(5):345–370. [PubMed: 10519688]

16. Matteucci ML, Anyarambhatla G, Rosner G, Azuma C, Fisher PE, Dewhirst MW, Needham D, Thrall DE. Hyperthermia increases accumulation of technetium-99m-labeled liposomes in feline sarcomas. Clin Cancer Res 2000;6(9):3748–3755. [PubMed: 10999769]

17. Hahn GM, Braun J, Har-Kedar I. Thermochemotherapy: Synergism between hyperthermia (42–43 degrees) and adriamycin (of bleomycin) in mammalian cell inactivation. Proc Natl Acad Sci U S A 1975;72(3):937–940. [PubMed: 48253]

18. Herman TS. Temperature dependence of adriamycin, cis-diamminedichloroplatinum, bleomycin, and 1,3-bis(2-chlor-oethyl)-1-nitrosourea cytotoxicity in vitro. Cancer Res 1983;43(2):517–520. [PubMed: 6184147]

19. Brewster AM, Hortobagyi GN, Broglio KR, Kau SW, Santa-Maria CA, Arun B, Buzdar AU, Booser DJ, Valero V, Bondy M, et al. Residual risk of breast cancer recurrence 5 years after adjuvant therapy. J Natl Cancer Inst 2008;100(16):1179–1183. [PubMed: 18695137]

20. Needham D, Anyarambhatla G, Kong G, Dewhirst MW. A new temperature-sensitive liposome for use with mild hyperthermia: Characterization and testing in a human tumor xenograft model. Cancer Res 2000;60(5):1197–1201. [PubMed: 10728674]

21. Ponce AM, Vujaskovic Z, Yuan F, Needham D, Dewhirst MW. Hyperthermia mediated liposomal drug delivery. Int J Hyperthermia 2006;22(3):205–213. [PubMed: 16754340]

22. Kong G, Anyarambhatla G, Petros WP, Braun RD, Colvin OM, Needham D, Dewhirst MW. Efficacy of liposomes and hyperthermia in a human tumor xenograft model: Importance of triggered drug release. Cancer Res 2000;60(24):6950–6957. [PubMed: 11156395]

23. Chen Q, Krol A, Wright A, Needham D, Dewhirst MW, Yuan F. Tumor microvascular permeability is a key determinant for antivascular effects of doxorubicin encapsulated in a temperature sensitive liposome. Int J Hyperthermia 2008;24(6):475–482. [PubMed: 18608573]

24. Mansour JC, Schwarz RE. Molecular mechanisms for individualized cancer care. J Am Coll Surg 2008;207(2):250–258. [PubMed: 18656055]

25. Basu S, Kumar R, Rubello D, Fanti S, Alavi A. PET imaging in neuroendocrine tumors: Current status and future prospects. Minerva Endocrinol 2008;33(3):257–275. [PubMed: 18846029]

26. Mohan HK, Miles KA. Cost-effectiveness of 99mTc-sesta-mibi in predicting response to chemotherapy in patients with lung cancer: Systematic review and meta-analysis. J Nucl Med 2009;50(3):376–381. [PubMed: 19223414]

27. Birdwell RL, Mountford CE, Iglehart JD. Molecular imaging of the breast. AJR Am J Roentgenol 2009;193(2):367–376. [PubMed: 19620433]

28. Sinha S, Sinha U. Recent advances in breast MRI and MRS. NMR Biomed 2009;22(1):3–16. [PubMed: 18654998]

29. Leach MO, Brindle KM, Evelhoch JL, Griffiths JR, Horsman MR, Jackson A, Jayson GC, Judson IR, Knopp MV, Maxwell RJ, et al. The assessment of antiangiogenic and antivascular therapies in

early-stage clinical trials using magnetic resonance imaging: Issues and recommendations. Br J Cancer 2005;92(9):1599–1610. [PubMed: 15870830]

30. Glunde KJM, Pathak AP, Artemov D, Bhujwalla ZM. Molecular and functional imaging of breast cancer. NMR Biomed 2008;22(1):92–103. [PubMed: 18792419]

31. Ikeda DM, Hylton NM, Kinkel K, Hochman MG, Kuhl CK, Kaiser WA, Weinreb JC, Smazal SF, Degani H, Viehweg P, et al. Development, standardization, and testing of a lexicon for reporting contrast-enhanced breast magnetic resonance imaging studies. J Magn Reson Imaging 2001;13(6): 889–895. [PubMed: 11382949]

32. Knopp MV, Weiss E, Sinn HP, Mattern J, Junkermann H, Radeleff J, Magener A, Brix G, Delorme S, Zuna I, et al. Pathophysiologic basis of contrast enhancement in breast tumors. J Magn Reson Imaging 1999;10(3):260–266. [PubMed: 10508285]

33. Knopp MV, von Tengg-Kobligk H, Choyke PL. Functional magnetic resonance imaging in oncology for diagnosis and therapy monitoring. Mol Cancer Ther 2003;2(4):419–426. [PubMed: 12700286]

34. Padhani AR, Hayes C, Assersohn L, Powles T, Makris A, Suckling J, Leach MO, Husband JE. Prediction of clinico-pathologic response of breast cancer to primary chemotherapy at contrast-enhanced MR imaging: Initial clinical results. Radiology 2006;239(2):361–374. [PubMed: 16543585]

35. Wedam SB, Low JA, Yang SX, Chow CK, Choyke P, Danforth D, Hewitt SM, Berman A, Steinberg SM, Liewehr DJ, et al. Antiangiogenic and antitumor effects of bevacizumab in patients with inflammatory and locally advanced breast cancer. J Clin Oncol 2006;24(5):769–777. [PubMed: 16391297]

36. Kuhl CK, Schild HH, Morakkabati N. Dynamic bilateral contrast-enhanced MR imaging of the breast: Trade-off between spatial and temporal resolution. Radiology 2005;236(3):789–800. [PubMed: 16118161]

37. Parker, GJM.; Buckley, DL. Tracer kinetic modelling for T1-weighted DCE-MRI. In: Jackson, A.; Buckley, DL.; Parker, GJM., editors. Dynamic Contrast Enhanced Magneric Resonance Imaging in Oncology. Berlin Heidelberg: Springer; 2005. p. 81-92.

38. Furman-Haran E, Schechtman E, Kelcz F, Kirshenbaum K, Degani H. Magnetic resonance imaging reveals functional diversity of the vasculature in benign and malignant breast lesions. Cancer 2005;104(4):708–718. [PubMed: 15971199]

39. Turnbull LW, Buckley DL, Turnbull LS, Liney GP, Knowles AJ. Differentiation of prostatic carcinoma and benign prostatic hyperplasia: Correlation between dynamic Gd-DTPA-enhanced MR imaging and histopathology. J Magn Reson Imaging 1999;9(2):311–316. [PubMed: 10077030]

40. O'Connor JP, Jackson A, Parker GJ, Jayson GC. DCE-MRI biomarkers in the clinical evaluation of antiangiogenic and vascular disrupting agents. Br J Cancer 2007;96(2):189–195. [PubMed: 17211479]

41. Roberts TP. Physiologic measurements by contrast-enhanced MR imaging: Expectations and limitations. J Magn Reson Imaging 1997;7(1):82–90. [PubMed: 9039597]

42. Beauregard DA, Thelwall PE, Chaplin DJ, Hill SA, Adams GE, Brindle KM. Magnetic resonance imaging and spectroscopy of combretastatin A4 prodrug-induced disruption of tumour perfusion and energetic status. Br J Cancer 1998;77(11):1761–1767. [PubMed: 9667644]

43. Mayr NA, Yuh WT, Magnotta VA, Ehrhardt JC, Wheeler JA, Sorosky JI, Davis CS, Wen BC, Martin DD, Pelsang RE, et al. Tumor perfusion studies using fast magnetic resonance imaging technique in advanced cervical cancer: A new noninvasive predictive assay. Int J Radiat Oncol Biol Phys 1996;36(3):623–633. [PubMed: 8948347]

44. Hawighorst H, Libicher M, Knopp MV, Moehler T, Kauffmann GW, Kaick G. Evaluation of angiogenesis and perfusion of bone marrow lesions: Role of semiquantitative and quantitative dynamic MRI. J Magn Reson Imaging 1999;10(3):286–294. [PubMed: 10508288]

45. Larson KB, Markham J, Raichle ME. Tracer-kinetic models for measuring cerebral blood flow using externally detected radiotracers. J Cereb Blood Flow Metab 1987;7(4):443–463. [PubMed: 3611204]

46. Brix G, Semmler W, Port R, Schad LR, Layer G, Lorenz WJ. Pharmacokinetic parameters in CNS Gd-DTPA enhanced MR imaging. J Comput Assist Tomogr 1991;15(4):621–628. [PubMed: 2061479]

47. Tofts PS, Berkowitz B, Schnall MD. Quantitative analysis of dynamic Gd-DTPA enhancement in breast tumors using a permeability model. Magn Reson Med 1995;33(4):564–568. [PubMed: 7776889]

48. Tofts PS. Modeling tracer kinetics in dynamic Gd-DTPA MR imaging. J Magn Reson Imaging 1997;7(1):91–101. [PubMed: 9039598]

49. Tofts PS, Brix G, Buckley DL, Evelhoch JL, Henderson E, Knopp MV, Larsson HB, Lee TY, Mayr NA, Parker GJ, et al. Estimating kinetic parameters from dynamic contrast-enhanced T(1)-weighted MRI of a diffusable tracer: Standardized quantities and symbols. J Magn Reson Imaging 1999;10(3):223–232. [PubMed: 10508281]

50. Tofts PS, Kermode AG. Measurement of the blood-brain barrier permeability and leakage space using dynamic MR imaging. 1. Fundamental concepts. Magn Reson Med 1991;17(2):357–367. [PubMed: 2062210]

51. Liu G, Rugo HS, Wilding G, McShane TM, Evelhoch JL, Ng C, Jackson E, Kelcz F, Yeh BM, Lee FT Jr, et al. Dynamic contrast-enhanced magnetic resonance imaging as a pharmacodynamic measure of response after acute dosing of AG-013736, an oral angiogenesis inhibitor, in patients with advanced solid tumors: Results from a phase I study. J Clin Oncol 2005;23(24):5464–5473. [PubMed: 16027440]

52. Padhani AR, Gapinski CJ, Macvicar DA, Parker GJ, Suckling J, Revell PB, Leach MO, Dearnaley DP, Husband JE. Dynamic contrast enhanced MRI of prostate cancer: Correlation with morphology and tumour stage, histological grade and PSA. Clin Radiol 2000;55(2):99–109. [PubMed: 10657154]

53. Stevenson JP, Rosen M, Sun W, Gallagher M, Haller DG, Vaughn D, Giantonio B, Zimmer R, Petros WP, Stratford M, et al. Phase I trial of the antivascular agent combretastatin A4 phosphate on a 5-day schedule to patients with cancer: Magnetic resonance imaging evidence for altered tumor blood flow. J Clin Oncol 2003;21(23):4428–4438. [PubMed: 14645433]

54. Dale BM, Jesberger JA, Lewin JS, Hillenbrand CM, Duerk JL. Determining and optimizing the precision of quantitative measurements of perfusion from dynamic contrast enhanced MRI. J Magn Reson Imaging 2003;18(5):575–584. [PubMed: 14579401]

55. Leach MO. Application of magnetic resonance imaging to angiogenesis in breast cancer. Breast Cancer Res 2001;3(1):22–27. [PubMed: 11300102]

56. Evelhohc, JLBT.; Chenevert, L., editors. Consensus recommendation for acquisition of dynamic contrast enhanced MRI data in oncology. Proceedings of the 8th Annual Meeting International Society for Magnetic Resonance in Medicine; Denver. 2000. p. 1439

57. Evelhoch JL. Key factors in the acquisition of contrast kinetic data for oncology. J Magn Reson Imaging 1999;10(3):254–259. [PubMed: 10508284]

58. Walker-Samuel S, Leach MO, Collins DJ. Evaluation of response to treatment using DCE-MRI: The relationship between initial area under the gadolinium curve (IAUGC) and quantitative pharmacokinetic analysis. Phys Med Biol 2006;51(14):3593–3602. [PubMed: 16825751]

59. Padhani AR. Functional MRI for anticancer therapy assessment. Eur J Cancer 2002;38(16):2116–2127. [PubMed: 12387837]

60. Ludemann L, Wust P, Gellermann J. Perfusion measurement using DCE-MRI: Implications for hyperthermia. Int J Hyperthermia 2008;24(1):91–96. [PubMed: 18214772]

61. Boehm T, Folkman J, Browder T, O'Reilly MS. Antiangiogenic therapy of experimental cancer does not induce acquired drug resistance. Nature 1997;390(6658):404–407. [PubMed: 9389480]

62. Rehman S, Jayson GC. Molecular imaging of antiangiogenic agents. Oncologist 2005;10(2):92–103. [PubMed: 15709211]

63. Folkman J. What is the evidence that tumors are angiogenesis dependent? J Natl Cancer Inst 1990;82(1):4–6. [PubMed: 1688381]

64. Pickles MD, Lowry M, Manton DJ, Gibbs P, Turnbull LW. Role of dynamic contrast enhanced MRI in monitoring early response of locally advanced breast cancer to neoadjuvant chemotherapy. Breast Cancer Res Treat 2005;91(1):1–10. [PubMed: 15868426]

65. Abraham DC, Jones RC, Jones SE, Cheek JH, Peters GN, Knox SM, Grant MD, Hampe DW, Savino DA, Harms SE. Evaluation of neoadjuvant chemotherapeutic response of locally advanced breast cancer by magnetic resonance imaging. Cancer 1996;78(1):91–100. [PubMed: 8646731]

66. Martincich L, Montemurro F, De Rosa G, Marra V, Ponzone R, Cirillo S, Gatti M, Biglia N, Sarotto I, Sismondi P, et al. Monitoring response to primary chemotherapy in breast cancer using dynamic contrast-enhanced magnetic resonance imaging. Breast Cancer Res Treat 2004;83(1):67–76. [PubMed: 14997056]

67. Julius T, Kemp SE, Kneeshaw PJ, Chaturvedi A, Drew PJ, Turnbull LW. MRI and conservative treatment of locally advanced breast cancer. Eur J Surg Oncol 2005;31(10):1129–1134. [PubMed: 15905068]

68. Wasser K, Klein SK, Fink C, Junkermann H, Sinn HP, Zuna I, Knopp MV, Delorme S. Evaluation of neoadjuvant chemotherapeutic response of breast cancer using dynamic MRI with high temporal resolution. Eur Radiol 2003;13(1):80–87. [PubMed: 12541113]

69. Drew PJ, Kerin MJ, Mahapatra T, Malone C, Monson JR, Turnbull LW, Fox JN. Evaluation of response to neoadjuvant chemoradiotherapy for locally advanced breast cancer with dynamic contrast-enhanced MRI of the breast. Eur J Surg Oncol 2001;27(7):617–620. [PubMed: 11669587]

70. Szabo BK, Aspelin P, Kristoffersen Wiberg M, Tot T, Bone B. Invasive breast cancer: Correlation of dynamic MR features with prognostic factors. Eur Radiol 2003;13(11):2425–2435. [PubMed: 12898176]

71. Chang YC, Huang CS, Liu YJ, Chen JH, Lu YS, Tseng WY. Angiogenic response of locally advanced breast cancer to neoadjuvant chemotherapy evaluated with parametric histogram from dynamic contrast-enhanced MRI. Phys Med Biol 2004;49(16):3593–3602. [PubMed: 15446790]

72. Baar J, Silverman P, Lyons J, Fu P, Abdul-Karim F, Ziats N, Wasman J, Hartman P, Jesberger J, Dumadag L, et al. A vasculature-targeting regimen of preoperative docetaxel with or without bevacizumab for locally advanced breast cancer: Impact on angiogenic biomarkers. Clin Cancer Res 2009;15(10):3583–3590. [PubMed: 19417018]

73. Johansen R, Jensen LR, Rydland J, Goa PE, Kvistad KA, Bathen TF, Axelson DE, Lundgren S, Gribbestad IS. Predicting survival and early clinical response to primary chemotherapy for patients with locally advanced breast cancer using DCE-MRI. J Magn Reson Imaging 2009;29(6):1300–1307. [PubMed: 19472387]

74. Wu F, Wang ZB, Cao YD, Chen WZ, Bai J, Zou JZ, Zhu H. A randomised clinical trial of high-intensity focused ultrasound ablation for the treatment of patients with localised breast cancer. Br J Cancer 2003;89(12):2227–2233. [PubMed: 14676799]

75. Wu F, Wang ZB, Zhu H, Chen WZ, Zou JZ, Bai J, Li KQ, Jin CB, Xie FL, Su HB. Extracorporeal high intensity focused ultrasound treatment for patients with breast cancer. Breast Cancer Res Treat 2005;92(1):51–60. [PubMed: 15980991]

76. Furusawa H, Namba K, Thomsen S, Akiyama F, Bendet A, Tanaka C, Yasuda Y, Nakahara H. Magnetic resonance-guided focused ultrasound surgery of breast cancer: Reliability and effectiveness. J Am Coll Surg 2006;203(1):54–63. [PubMed: 16798487]

77. Craciunescu OI, Blackwell KL, Jones EL, Macfall JR, Yu D, Vujaskovic Z, Wong TZ, Liotcheva V, Rosen EL, Prosnitz LR, et al. DCE-MRI parameters have potential to predict response of locally advanced breast cancer patients to neoadjuvant chemotherapy and hyperthermia: A pilot study. Int J Hyperthermia 2009;25(6):405–415. [PubMed: 19657852]

78. Craciunescu, OI.; Jones, EL.; Blackwell, KL.; Wong, TZ.; Rosen, EL.; Vujaskovic, Z.; MacFall, JR.; Liotcheva, V.; Lora-Michels, M.; Prosnitz, LP., et al., editors. SPIE. San Jose: SPIE Publishing; 2005. Characterizing tumor changes during neoadjuvant treatment of locally advanced breast cancer patients (LABC) using dynamic-enhanced magnetic resonance imaging (DCE-MRI).

79. Mukherji SK, Chenevert TL, Castillo M. Diffusion-weighted magnetic resonance imaging. J Neuroophthalmol 2002;22(2):118–122. [PubMed: 12131474]

80. Chenevert TL, Meyer CR, Moffat BA, Rehemtulla A, Mukherji SK, Gebarski SS, Quint DJ, Robertson PL, Lawrence TS, Junck L, et al. Diffusion MRI: A new strategy for assessment of cancer therapeutic efficacy. Mol Imaging 2002;1(4):336–343. [PubMed: 12926229]

81. Sinha S, Sinha U. Functional magnetic resonance of human breast tumors: Diffusion and perfusion imaging. Ann N Y Acad Sci 2002;980:95–115. [PubMed: 12594084]

82. Van Zijl PC, Moonen CT, Faustino P, Pekar J, Kaplan O, Cohen JS. Complete separation of intracellular and extra-cellular information in NMR spectra of perfused cells by diffusion-weighted spectroscopy. Proc Natl Acad Sci U S A 1991;88(8):3228–3232. [PubMed: 2014244]

83. Horsfield MA, Barker GJ, McDonald WI. Self-diffusion in CNS tissue by volume-selective proton NMR. Magn Reson Med 1994;31(6):637–644. [PubMed: 8057816]

84. Niendorf T, Dijkhuizen RM, Norris DG, van Lookeren Campagne M, Nicolay K. Biexponential diffusion attenuation in various states of brain tissue: Implications for diffusion-weighted imaging. Magn Reson Med 1996;36(6):847–857. [PubMed: 8946350]

85. Chenevert TL, Stegman LD, Taylor JM, Robertson PL, Greenberg HS, Rehemtulla A, Ross BD. Diffusion magnetic resonance imaging: An early surrogate marker of therapeutic efficacy in brain tumors. J Natl Cancer Inst 2000;92(24):2029–2036. [PubMed: 11121466]

86. Kauppinen RA. Monitoring cytotoxic tumour treatment response by diffusion magnetic resonance imaging and proton spectroscopy. NMR Biomed 2002;15(1):6–17. [PubMed: 11840548]

87. Lyng H, Haraldseth O, Rofstad EK. Measurement of cell density and necrotic fraction in human melanoma xenografts by diffusion weighted magnetic resonance imaging. Magn Reson Med 2000;43(6):828–836. [PubMed: 10861877]

88. Guo Y, Cai YQ, Cai ZL, Gao YG, An NY, Ma L, Mahankali S, Gao JH. Differentiation of clinically benign and malignant breast lesions using diffusion-weighted imaging. J Magn Reson Imaging 2002;16(2):172–178. [PubMed: 12203765]

89. Ross BD, Moffat BA, Lawrence TS, Mukherji SK, Gebarski SS, Quint DJ, Johnson TD, Junck L, Robertson PL, Muraszko KM, et al. Evaluation of cancer therapy using diffusion magnetic resonance imaging. Mol Cancer Ther 2003;2(6):581–587. [PubMed: 12813138]

90. Mardor Y, Roth Y, Ochershvilli A, Spiegelmann R, Tichler T, Daniels D, Maier SE, Nissim O, Ram Z, Baram J, et al. Pretreatment prediction of brain tumors' response to radiation therapy using high b-value diffusion-weighted MRI. Neoplasia 2004;6(2):136–142. [PubMed: 15140402]

91. Dzik-Jurasz A, Domenig C, George M, Wolber J, Padhani A, Brown G, Doran S. Diffusion MRI for prediction of response of rectal cancer to chemoradiation. Lancet 2002;360(9329):307–308. [PubMed: 12147376]

92. Kremser C, Judmaier W, Hein P, Griebel J, Lukas P, de Vries A. Preliminary results on the influence of chemoradiation on apparent diffusion coefficients of primary rectal carcinoma measured by magnetic resonance imaging. Strahlenther Onkol 2003;179(9):641–649. [PubMed: 14628131]

93. Hein PA, Kremser C, Judmaier W, Griebel J, Pfeiffer KP, Kreczy A, Hug EB, Lukas P, DeVries AF. Diffusion-weighted magnetic resonance imaging for monitoring diffusion changes in rectal carcinoma during combined, pre-operative chemoradiation: Preliminary results of a prospective study. Eur J Radiol 2003;45(3):214–222. [PubMed: 12595106]

94. DeVries AF, Kremser C, Hein PA, Griebel J, Krezcy A, Ofner D, Pfeiffer KP, Lukas P, Judmaier W. Tumor microcirculation and diffusion predict therapy outcome for primary rectal carcinoma. Int J Radiat Oncol Biol Phys 2003;56(4):958–965. [PubMed: 12829130]

95. Cui Y, Zhang XP, Sun YS, Tang L, Shen L. Apparent diffusion coefficient: Potential imaging biomarker for prediction and early detection of response to chemotherapy in hepatic metastases. Radiology 2008;248(3):894–900. [PubMed: 18710982]

96. Harry VN, Semple SI, Gilbert FJ, Parkin DE. Diffusion-weighted magnetic resonance imaging in the early detection of response to chemoradiation in cervical cancer. Gynecol Oncol 2008;111(2): 213–220. [PubMed: 18774597]

97. Okuma T, Matsuoka T, Yamamoto A, Hamamoto S, Nakamura K, Inoue Y. Assessment of early treatment response after CT-guided radiofrequency ablation of unre-sectable lung tumours by diffusion-weighted MRI: A pilot study. Br J Radiol 2009;82(984):989–994. [PubMed: 19470575]

98. Reichardt W, Juettner E, Uhl M, Elverfeldt DV, Kontny U. Diffusion-weighted imaging as predictor of therapy response in an animal model of Ewing sarcoma. Invest Radiol 2009;44(5): 298–303. [PubMed: 19346963]

99. Whittaker CS, Coady A, Culver L, Rustin G, Padwick M, Padhani AR. Diffusion-weighted MR imaging of female pelvic tumors: A pictorial review. Radiographics 2009;29(3):759–74. discussion 74–78. [PubMed: 19448114]

100. Theilmann RJ, Borders R, Trouard TP, Xia G, Outwater E, Ranger-Moore J, Gillies RJ, Stopeck A. Changes in water mobility measured by diffusion MRI predict response of metastatic breast cancer to chemotherapy. Neoplasia 2004;6(6):831–837. [PubMed: 15720810]

101. Pickles MD, Gibbs P, Lowry M, Turnbull LW. Diffusion changes precede size reduction in neoadjuvant treatment of breast cancer. Magn Reson Imaging 2006;24(7):843–847. [PubMed: 16916701]

102. Yankeelov TE, Lepage M, Chakravarthy A, Broome EE, Niermann KJ, Kelley MC, Meszoely I, Mayer IA, Herman CR, McManus K, et al. Integration of quantitative DCE-MRI and ADC mapping to monitor treatment response in human breast cancer: Initial results. Magn Reson Imaging 2007;25(1):1–13. [PubMed: 17222711]

103. Ma B, Meyer CR, Pickles MD, Chenevert TL, Bland PH, Galban CJ, Rehemtulla A, Turnbull LW, Ross BD. Voxel-by-voxel functional diffusion mapping for early evaluation of breast cancer treatment. Inf Process Med Imaging 2009;21:276–287. [PubMed: 19694270]

104. Chen J, Daniel BL, Diederich CJ, Bouley DM, van den Bosch MA, Kinsey AM, Sommer G, Pauly KB. Monitoring prostate thermal therapy with diffusion-weighted MRI. Magn Reson Med 2008;59(6):1365–1372. [PubMed: 18506801]

105. Ohira T, Okuma T, Matsuoka T, Wada Y, Nakamura K, Watanabe Y, Inoue Y. FDG-MicroPET and diffusion-weighted MR image evaluation of early changes after radiofrequency ablation in implanted VX2 tumors in rabbits. Cardiovasc Intervent Radiol 2009;32(1):114–120. [PubMed: 18696151]

106. Liney GP, Gibbs P, Hayes C, Leach MO, Turnbull LW. Dynamic contrast-enhanced MRI in the differentiation of breast tumors: User-defined versus semi-automated region-of-interest analysis. J Magn Reson Imaging 1999;10(6):945–949. [PubMed: 10581507]

107. Schnall MD. An overview of interpretation strategies for breast MR imaging. Magn Reson Imaging Clin N Am 2001;9(2):289–294. v–vi. [PubMed: 11493419]

108. Kuhl CK, Mielcareck P, Klaschik S, Leutner C, Wardelmann E, Gieseke J, Schild HH. Dynamic breast MR imaging: Are signal intensity time course data useful for differential diagnosis of enhancing lesions? Radiology 1999;211(1):101–110. [PubMed: 10189459]

109. Helbich TH. Contrast-enhanced magnetic resonance imaging of the breast. Eur J Radiol 2000;34(3):208–219. [PubMed: 10927162]

110. Hayes C, Padhani AR, Leach MO. Assessing changes in tumour vascular function using dynamic contrast-enhanced magnetic resonance imaging. NMR Biomed 2002;15(2):154–163. [PubMed: 11870911]

111. Parker GJ, Suckling J, Tanner SF, Padhani AR, Revell PB, Husband JE, Leach MO. Probing tumor microvascularity by measurement, analysis and display of contrast agent uptake kinetics. J Magn Reson Imaging 1997;7(3):564–574. [PubMed: 9170043]

112. Tanner C, Schnabel JA, Hill DL, Hawkes DJ, Degenhard A, Leach MO, Hose DR, Hall-Craggs MA, Usiskin SI. Quantitative evaluation of free-form deformation registration for dynamic contrast-enhanced MR mammography. Med Phys 2007;34(4):1221–1233. [PubMed: 17500454]

113. Li X, Dawant BM, Welch EB, Chakravarthy AB, Freehardt D, Mayer I, Kelley M, Meszoely I, Gore JC, Yankeelov TE. A nonrigid registration algorithm for longitudinal breast MR images and the analysis of breast tumor response. Magn Reson Imaging 2009;27(9):1258–1270. [PubMed: 19525078]

114. Ludemann L, Prochnow D, Rohlfing T, Franiel T, Warmuth C, Taupitz M, Rehbein H, Beyersdorff D. Simultaneous quantification of perfusion and permeability in the prostate using dynamic contrast-enhanced magnetic resonance imaging with an inversion-prepared dual-contrast sequence. Ann Biomed Eng 2009;37(4):749–762. [PubMed: 19169821]

115. Matsumoto S, Yasui H, Batra S, Kinoshita Y, Bernardo M, Munasinghe JP, Utsumi H, Choudhuri R, Devasahayam N, Subramanian S, et al. Simultaneous imaging of tumor oxygenation and microvascular permeability using Overhauser enhanced MRI. Proc Natl Acad Sci U S A 2009;106(42):17898–17903. [PubMed: 19815528]
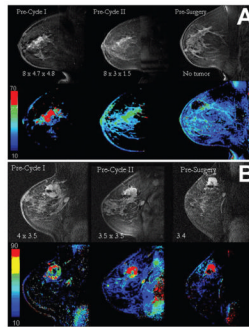
Figure 1.
DCE-MRI images (first row) of one sagittal image through the centre of the tumour for a patient that responded (A) and did not respond to treatment (B), respectively, pre cycle I, pre cycle II and before surgery. On each image, the size of the lesion based on MR is given. The wash-in parametric maps are shown in the second row. The scales refer to wash-in parameter values, no units.
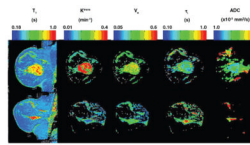
Figure 2.
Pre-treatment and post-treatment parametric mappings of the central slice of the tumour from a representative patient. The top row displays the pre-treatment T_1, K_{trans}, v_e, τ_i and ADC parametric maps, respectively, while the bottom row shows the corresponding post-treatment maps. In addition to the reduction in tumour size seen in all mappings, relative changes in the distribution of each parameter are visible. Most noticeable is the large drop in the fraction of red pixels on the K^{trans} map, indicating a decrease in tumour vessel perfusion and/or permeability; the increase in the ADC map indicates a more geometrically favourable water diffusion environment (reproduced with permission from Yankeelov et al. [102]).